



Design, characterization and evaluation of gelatin/ carboxymethyl cellulose hydrogels for effective delivery of ciprofloxacin

Fariha Sahar¹ · Amina Riaz³ · Nadia Shamshad Malik²  · Nitasha Gohar² ·
Ayesha Rasheed³ · Ume Ruqia Tulain⁴ · Alia Erum⁴ · Kashif Barkat⁵ ·
Syed Faisal Badshah⁵ · Sayyed Ibrahim Shah⁶

Received: 8 August 2022 / Revised: 5 November 2022 / Accepted: 4 December 2022 /
Published online: 23 December 2022

© The Author(s), under exclusive licence to Springer-Verlag GmbH Germany, part of Springer Nature 2022

Abstract

The present work is to synthesize and characterize pH-sensitive gelatin/carboxymethyl cellulose (gelatin/CMC) hydrogels crosslinked with glutaraldehyde (GA). The effect of polymer ratio and crosslinking on dynamic swelling, equilibrium swelling and in vitro release pattern of model drug ciprofloxacin hydrochloride was investigated. Swelling and release studies were conducted in phosphate buffer solutions of various pH ranging from 1.2, 5.5 and 7.4. Hydrogels were characterized by FTIR (Fourier transform infrared spectroscopy), XRD (X-ray diffraction), SEM scanning electron microscopy and DSC (differential scanning calorimetry). The drug release data were fitted to various models to determine best fit release model. Drug-loaded hydrogels were further subjected to antioxidant, antibacterial and antifungal assays to assess the pharmacological profile of encapsulated drug, whereas cytotoxicity of prepared hydrogel was also evaluated. The results showed that maximum swelling and consequent highest release of drug occurred at pH 1.2 where gelatin was mainly responsible for swelling and release characteristics. The results of FTIR and XRD proved the crosslinking of polymers and compatibility of drug with polymers, whereas DSC confirmed the molecular dispersion of drug in the polymeric network. Release pattern of drug was zero order and the release of drug occurred through non-Fickian diffusion. The results obtained from various biological assays were sufficient to verify the hydrogels as potential drug carrier. Overall the results demonstrated the prepared hydrogels as a favourable drug carrier to achieve controlled drug release for different antimicrobial agents.

Keywords Gelatin · Carboxymethyl cellulose · Hydrogels · Antifungal ·
Antibacterial

✉ Nadia Shamshad Malik
nadiashamshad@gmail.com

Extended author information available on the last page of the article

Introduction

The emergence of opportunistic pathogens and continuous resistance to antimicrobials has limited the global efforts to treat diseases and achieve health-related sustainable development goals, worldwide [1]. Antimicrobial resistance (AMR) creates a rising hazard to community wellbeing and the provision of health care. Among developing countries, AMR is often considered as being ‘mushrooming and often neglected’ [2]. The WHO recently recommended Pakistan as a global hotspot for the surfacing and multiplication of AMR. Thus, antimicrobial resistance is a neglected global crisis that requires imperative awareness and action [3].

Ciprofloxacin hydrochloride is a water-soluble, broad spectrum and second-generation fluoroquinolone antibiotic and has good antibacterial activity against gram-negative and gram-positive bacteria. Its half-life is 3 to 5 h and minimum inhibitory concentration (MIC) is 1 to 2 $\mu\text{g/mL}$. It is effectively used in various infections and has been used as a single agent for the treatment of pneumonia due to its high therapeutic efficacy. Besides, the administration of ciprofloxacin has been associated with a number of rare but serious side effects including arthritis, severe liver injury (hepatitis), loss of vision, double vision, drug fever, acute pancreatitis and so on. Therefore, designing and development of a controlled release drug delivery system (CRDDS) for ciprofloxacin is desirable. In recent years, the application of polymeric drug delivery system has been expanded to formulate new drug delivery systems, which are capable of improving the pharmacokinetics and therapeutic outcomes of already available drugs including antimicrobial effects [4]. The utilization of polymeric carriers for conservative antibiotics has been confirmed to augment their antimicrobial activity against drug-resistant microbial strains and diminish their adverse effects [5, 6]. Therefore, there is an urgent need in developing new therapeutic approaches showing potential to surmount the emergent threat of drug resistance. Among polymeric technology, hydrogels are considered as excellent carriers to increase the bioavailability, greater retention time and decreasing the undesirable side effects. Moreover, these polymeric networks have further advantage of high encapsulation efficiency and controlled delivery of encapsulated therapeutic moiety [7, 8].

Hydrogels are crosslinked polymeric networks having ability to swell by absorbing liquid without losing their structural integrity [9]. Swelling ability of hydrogels can be modified to desirable extent by altering the monomeric/polymeric concentration and crosslinking density [10]. Hydrogels have gained immense interest in pharmaceutical fields especially for controlled drug delivery. Synthesis and characterization of hydrogels is a rapidly growing research area, and many natural as well as synthetic polymers have been utilized for the said purpose [11]. Natural polymers are used extensively because of their high-water content (similarity with natural tissues), non-toxicity, non-immunogenicity and biodegradability.

Gelatin is a water-soluble protein obtained from thermal denaturation of collagen [12]. Degradation of triple helix structure of native collagen results in formation of single-stranded chains of gelatin [13]. When aqueous solution of gelatin is cooled at temperature below 35 °C, the triple helix structure of collagen is partially resumed

and causes the formation of thermally reversible gels [14]. Gelatin is comparatively cheaper and readily available material. It is amphoteric in nature having both acidic and basic functional groups. Ratio between amino (basic) and carboxylic (acidic) groups determines the isoelectric pH of gelatin, i.e. 4.6. Low melting point (below 34 °C) of gelatin is the main drawback due to which it cannot be used at higher temperatures that cause breaking of secondary bonds and destruction of the physical network [15]. Thus, low thermal and mechanical stability has limited the use of gelatin. Chemical crosslinking of gelatin chains improves its thermal stability, and numerous crosslinking agents such as glutaraldehyde, carbodiimide, formaldehyde and chondroitin sulphate have been used for this purpose [16, 17].

Another way to stabilize gelatin chains is its mixing with another natural polymer such as sodium salt of carboxymethyl cellulose (CMC). CMC is anionic cellulose ether with various useful properties such as non-toxicity, biodegradability, biocompatibility and excellent water absorbency [18, 19]. Degree of substitution (DS) of CMC varies according to its synthesis procedure. Low DS of CMC causes a higher swelling ability and lower gel strength. For increasing the gel strength, a mixture of gelatin and CMC had been used for preparation of hydrogel [20].

Glutaraldehyde (GA) was selected as crosslinker. Carbonyl group of GA reacts with unprotonated amino group of gelatin and hydroxyl group of CMCs to form a 3-D network [21]. Although crosslinking agents improve the mechanical strength of hydrogel, on the other hand these also decrease the absorbing capacity of hydrogel leading to a decrease in drug loading and release. Therefore, optimum concentration of crosslinking agent is necessary [22].

In the present study, we fabricated pH-sensitive hydrogel based on gelatin and CMC crosslinked with GA. The drug release profile of developed formulation was investigated by varying formulation reactants concentration and pH of the medium. Based on drug release profile, the optimal formulation was elected. Structural features of hydrogel were characterized by Fourier transform infrared spectroscopy (FTIR), scanning electron microscope (SEM), differential scanning calorimeter (DSC), porosity, sol–gel analysis, molecular weight between crosslinks (Mc) and volume fraction of polymer ($V_{2,s}$). Different models, for example zero order, first order, Higuchi and Korsmeyer–Peppas model, were applied to analyse the release pattern of drug. The effect of varying concentrations of polymers and crosslinker on swelling and release behaviour of hydrogel was also evaluated. In the end, various biological assays including cytotoxicity, antioxidant, antibacterial and antifungal were performed to confirm the safety and efficacy of prepared hydrogels.

Materials and method

Materials

Ciprofloxacin was gifted for conducting research work by Getz Pharma (Pvt) Ltd. (Karachi, Pakistan). The polymers gelatin and carboxymethyl cellulose were purchased from Sigma-Aldrich (UK). The analytical grade crosslinker glutaraldehyde

was also obtained from Fluka. Distilled water was prepared at research laboratory of Pharmacy Department, Women University, Multan, Pakistan.

Preparation of Gelatin/CMC based hydrogels

The gelatin/CMC hydrogels were synthesized by solution reaction of polymers and a series of hydrogels were prepared [23]. Weighed amount of gelatin was dissolved in 3% solution of acetic acid at 45 °C by adding gelatin powder in parts to acetic acid with constant stirring, until homogenous mixture was obtained. Acetic acid was used as catalyst of reaction to enhance the function of crosslinker. CMC solution was prepared by mixing weighed amount of CMC in distilled water in the same way as gelatin. Then both solutions were mixed together and stirred until clear solution was obtained. Glutaraldehyde, as a crosslinker, was added dropwise while stirring and finally distilled water was added to make final weight of solution 50 g. The prepared solution was poured into glass tubes to start reaction. Tubes were deoxygenated by nitrogen gas for 15 to 20 min to remove bubbles, and then, tubes were fitted with lids and placed at room temperature for 72 h. After completion of reaction and gelation, cylindrical hydrogels were taken out from glass tubes and divided into discs of 6 mm length. Next, hydrogel discs were washed with ethanol–water mixture (70:30) to remove unreacted polymer for one week.

This process continued up to a stable value of pH was obtained. Hydrogel was further dried in a lyophilizer at –55 °C until drying equilibrium. Chemical compositions of developed hydrogel are shown in Table 1, while schematic representation of reactants and possible grafted structure of hydrogel are shown in Fig. 1.

Drug loading

For drug loading, discs were soaked in 1% (w/v) aqueous solution of ciprofloxacin hydrochloride. Discs were allowed to remain in drug solution until achievement of constant weight. Loaded hydrogels discs were removed from the drug solution and flushed

Table 1 Different formulations of gelatin/CMC hydrogel

Samples	Gelatin/100 g solution	CMC/100 g solution	GA/100 g solution
S1	14	0.85	3.65
S2	14	0.95	3.65
S3	14	1.05	3.65
S4	13	0.95	3.65
S5	15	0.95	3.65
S6	17	0.95	3.65
S7	14	0.95	3.50
S8	14	0.95	3.75
S9	14	0.95	4.00

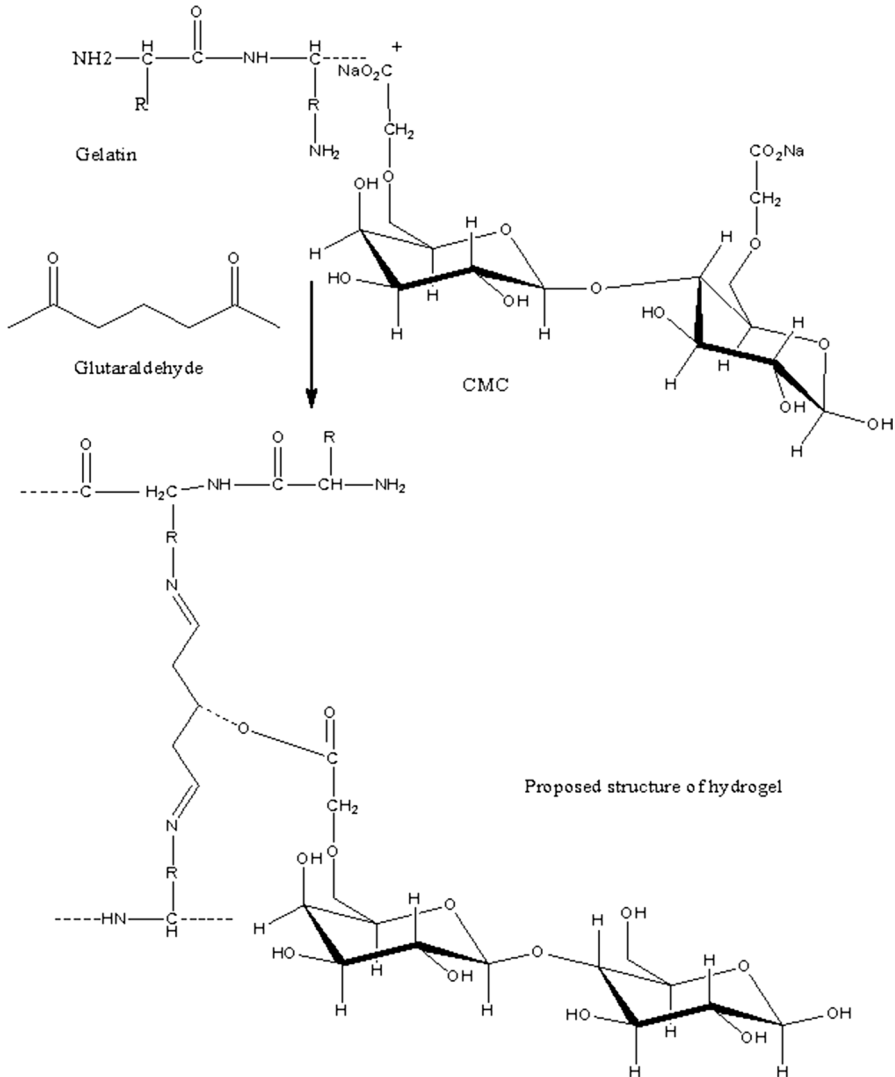


Fig. 1 Proposed structure of gelatin/CMC hydrogel crosslinked with GA

with distilled water carefully to eliminate any residual mass of drug on the exterior surface of the hydrogel discs. They were then subjected to freeze-drying using the lyophilizer [24].

Structural parameters of hydrogels

Diffusion coefficient

Diffusion of a substance across a unit area by concentration gradient in unit time is called diffusion coefficient. It is dependent on nature and segmental mobility of polymer [25].

It is calculated by following formula

$$D = \pi \left(\frac{h \cdot \theta}{4 \cdot q_{eq}} \right)^2 \quad (1)$$

where q_{eq} is equilibrium swelling of hydrogel disc, θ represent slope of linear part of swelling curves and h is the thickness of hydrogel disc before swelling.

Physicochemical characterization of gelatin/CMC hydrogel

The prominent parameters that evaluate the structure and characteristics of hydrogels in swollen state are volume fraction of polymer in the swollen state $V_{2,s}$, molecular weight among crosslinking junctions M_c , solvent interaction parameters χ , the number of links between two crosslinks (N), FTIR spectroscopic analysis, XRD (X-ray diffraction), SEM (Scanning electron microscopy) and DSC (Differential scanning calorimetry).

Volume fraction of polymer ($V_{2,s}$)

$V_{2,s}$ is the capacity of hydrogel to which it can absorb and retain maximum fluid [26].

$$V_{2,s} = \left[1 + \frac{d_p}{d_s} \left(\frac{M_a}{M_b} - 1 \right) \right]^{-1} \quad (2)$$

In this equation d_p and d_s are the densities of the polymer and solvent, M_b and M_a are the masses of the dry and swollen polymers, respectively.

Determination of average molecular weight between crosslinks (M_c)

Extent of crosslinking of polymer network can be determined by M_c . It is obtained by following equation [27].

$$M_c = \frac{d_p V_s \left(V_{2,s}^{1/3} - V_{2,s} / 2 \right)}{\ln \left(1 - V_{2,s} \right) + V_{2,s} + \chi V_{2,s}^2} \quad (3)$$

where d_p and d_s are the densities of the polymer and solvent, respectively. V_s is the molar volume of the solvent and χ is the Flory–Huggins polymer solvent interaction parameters.

Determination of solvent interaction parameters (χ)

χ can be calculated by Flory–Huggins theory. According to this theory [28],

$$\chi = \frac{\ln(1 - V_{2,s}) + V_{2,s}}{V_{2,s}^2} \tag{4}$$

where $V_{2,s}$ is volume fraction of swollen gel in the equilibrium state.

Number of links between crosslinks (N)

Data of M_c were utilized to determine N . Equation is given below [29];

$$N = \frac{2M_c}{M_r} \tag{5}$$

M_r is the molar mass of the repeating unit. It is calculated by the following equation;

$$M_r = \frac{m_{GEL}M_{GEL} + m_{CMC}M_{CMC} + m_{GA}M_{GA}}{m_{GEL} + m_{CMC} + m_{GA}} \tag{6}$$

where m_{GEL} , m_{CMC} and m_{GA} are the masses of gelatin, carboxymethyl cellulose and glutaraldehyde, respectively. M_{GEL} , M_{CMC} and M_{GA} are the molar masses of gelatin, carboxymethyl cellulose and glutaraldehyde.

Sol–gel fraction

Amount of uncrosslinked or unreacted polymer is determined by analysing sol–gel fraction. Un-washed samples were used. Discs were further divided into pieces. They were dried at room temperature and then in vacuum oven at 45 °C until constant weight was obtained. Apparatus used for extraction of discs was Soxhelt extractor and it was done for 4 h using deionized water as solvent to remove the uncrosslinked polymer from the hydrogel disc. After extraction, samples were again vacuum-dried at 45 °C until constant weight was obtained. Weights of dry and extracted gel were used to calculate sol–gel fraction. Equation is given below [30].

$$\text{Sol fraction (\%)} = \left[\frac{W_o - W_1}{W_o} \right] \times 100 \tag{7}$$

$$\text{Gel fraction (\%)} = 100 - \text{Sol fraction} \tag{8}$$

Porosity measurement

Weight of dry hydrogels was measured and dry disc was placed in absolute ethanol overnight. Then again weight of discs was measured at end. Density, volume and mass of hydrogel were used to calculate porosity. Equation is given below [31].

$$\text{Porosity} = \frac{(M_2 - M_1)}{\rho V} \quad (9)$$

where M_1 and M_2 are the mass of hydrogel before and after immersion in ethanol, respectively, ρ is the density of absolute ethanol and V is the volume of the hydrogel.

FTIR spectroscopic analysis

Hydrogel discs were broken and powdered in pestle and mortar. The resulted material was added into potassium bromide and dried at 40 °C. The mixture was pressurized with 65 kN pressure by using pressure gauge (Shimadzu) for 2 min and squashed to partially transparent disc of 12 mm size. FTIR spectrometer with specification of FTIR 8400 S, Shimadzu, was used. The FTIR spectrum was recorded and wavelength range of 4000–400 cm^{-1} was used.

Differential scanning calorimetry (DSC)

DSC unit (Shimadzu DSC – 50) was used for this purpose. Samples were heated in a closed aluminium pan at the rate of 10 °C/ minute. Nitrogen gas was used for purging at flowing rate of 20 mL/min.

X-ray diffraction (XRD)

X-ray diffraction (XRD) for drug-loaded and -unloaded hydrogel was performed using Bruker D8 Discover (Germany) apparatus. Measurement conditions included target ($\text{CuK}\alpha$), voltage (35 kV) and current (35 mA). Eva software was used for the data processing (Evaluation Package Bruker, Germany). Patterns were obtained using scan speed of 4 degree/minute with 2θ between 5 and 80°.

Scanning electron microscopy

Surface morphology of synthesized hydrogels was observed using SEM. Samples were gold coated and images were taken using S3400-N Hitachi model under various resolutions.

Swelling measurement

Dynamic swelling study of hydrogels was carried out in USP phosphate buffers of various pH values, i.e. 1.2, 5.5 and 7.4, whereas ionic strength was kept constant.

First of all, weight of dry disc was noted and then discs were placed in solution of desired pH values. Samples were removed from solution repeatedly at specific time interval, weighed after blotting using paper and put in the same buffer again. Swelling ratio was calculated by dividing weight of swollen gel to the weight of dry disc. Equation is given below [32].

$$q = \frac{W_t}{W_d} \quad (10)$$

where $W_{t\text{is}}$ weight of swollen gel at time t and W_d is the initial weight of dry gel.

For equilibrium swelling studies, discs were allowed to remain in buffer solution for swelling until constant weight was gained. It took approximately 15 days. At lower pH, discs absorbed more water and became fragile. So, discs were handled carefully to avoid damage. Equation to calculate equilibrium swelling ratio is given below [33].

$$q_{(Eq)} = \frac{W_h}{W_d} \quad (11)$$

where W_h is the weight of swollen gel at equilibrium and W_d is the initial weight of dry gel.

Drug entrapment efficiency (DEE) and drug release behaviour

For the investigation of drug entrapment efficiency of developed hydrogels, drug-loaded hydrogel discs were grinded thoroughly in a mortar and pestle to make powder. These powdered hydrogels were added to phosphate buffer solution of pH 7.4 maintained at 37 ± 0.5 °C for 24 h with continuous stirring. After specified time, centrifugation of above solution was conducted at 3000 rpm for 12 min. The supernatant layer was removed and filtered through 0.45- μm filter paper. Drug assay was conducted using UV–visible spectrophotometer (Shimadzu, Japan; Model–UV 1800).

Release study of drug was carried out by dissolution test in vitro. Dissolution apparatus equipped with UV–VIS spectrophotometer was used. For this purpose a series of phosphate buffer solutions (PBS) of various pH values, i.e. 1.2, 5.5 and 7.4, were prepared and used as dissolution medium. A total of 500 mL of dissolution medium was used and drug-loaded discs were dipped in it. Teflon coated stirring bar was used to keep uniform concentration of drug in solution. Stirring rate was 100 rpm and temperature was set at 37 °C. After fixed time intervals, 5 ml of solution was taken and replaced with fresh medium each time. The removed solution was analysed by UV–visible spectrophotometer to determine concentration of drug. Release study of drug was done for 12 h and percentage drug release was calculated with help of standard curve. Drug release data were fitted to various models including zero order, first order, Higuchi and Korsmeyer–Peppas models.

$$\text{Zero – order kinetics } F_t = K_0 t \quad (12)$$

where F_t is the amount of drug released in time t and K_0 is the apparent rate constant for zero-order release.

$$\text{First order kinetics } \ln(1 - F) = -K_1 t \quad (13)$$

where F indicates the amount of drug released in time t and k_1 is the first-order release rate constant.

$$\text{Higuchi model } F = K_2 t^{1/2} \quad (14)$$

F indicates the amount of drug released in time t and K_2 is Higuchi constant. This model is based on several hypotheses: (I) solubility of drug is less than initial quantity of drug in matrix (II) drug diffuses in one direction only

$$\text{Korsmeyer – Peppas model } M_t/M_\infty = K_3 t^n \quad (15)$$

where M_t is mass of water absorbed in time t and M_∞ is mass of water absorbed at equilibrium. K_3 is constant incorporating the structural and geometric characteristics of the gels and n is the release exponent. A value of $n=0.45$ indicates Fickian release, whereas value of $n > 0.45$ and < 1 indicates non-Fickian release [34]. This equation of Korsmeyer–Peppas model demonstrates the rate of release of drug in terms of relaxation-controlled and the diffusion-controlled transport process.

Biological evaluation

On the basis of maximum drug entrapment efficiency and in vitro cumulative drug release, one optimized hydrogel formulation was chosen for biological evaluation. Antioxidant, cytotoxic, antibacterial and antifungal assays were conducted for biological evaluation.

Antioxidant assay

Antioxidant activity of the optimized hydrogel was measured by taking 2 mL of 100 μM 2,2-diphenyl-1-picrylhydrazyl (DPPH) dissolved in methanol which is then mixed with 2 mL of various concentrations (0–20 $\mu\text{g/mL}$) of optimized hydrogel [35]. The obtained solution was incubated in dark for 30 min. Ascorbic acid was used as a positive control. Absorption of samples at 517 nm was checked with a spectrophotometer (Agilent 8453), and antioxidant activity was determined by using the following equation [36].

$$\text{Percentage scavenging} = \left(\frac{\text{Absorbance of control} - \text{absorbance of test sample}}{\text{Absorbance of control}} \right) * 100 \quad (16)$$

Cytotoxicity assay

We made use of brine shrimp (*Artemia salina*) to study the toxicity of optimized hydrogel at selective concentrations from 0 to 20 $\mu\text{g}/\text{mL}$ [37]. Dried cysts of brine shrimp eggs (Sera, Heidelberg, Germany) were placed in a bottle containing artificial sea water which was prepared by dissolving 35 g of sodium chloride in 1 L of distilled water. After 48 h incubation at room temperature 37 °C under conditions of strong aeration and continuous illuminations, the larvae (nauplii) hatched within 48 h. The evaluation of cytotoxicity of optimized hydrogel in brine shrimp was performed. The assay was carried out on larvae of brine shrimp (*A. salina* Leach.). When the shrimp larvae are ready, 5 mL of the artificial sea-water and 5 mL of hydrogel solution were added to each test tube and 10 brine shrimps were introduced into each tube. Thus, there were a total of 50 shrimps per dilution. The artificial sea water up to 10 mL per test tube is control. The test tubes were left uncovered under the lamp. The number of surviving shrimps was counted and recorded after 24 h. The percentage viability (% V) was calculated by dividing the number of alive nauplii by the total number and then multiplied by 100% as mentioned in below equation [38]

$$\text{Percentage Viability} = \left[\frac{\text{test} - \text{control}}{\text{control}} \right] \times 100 \quad (17)$$

Antibacterial assay

Both gram-negative (*P. aeruginosa*, *Klebsiella* and *E. coli*) and gram-positive (*S. aureus* and *S. pneumoniae*) bacteria were used to study the antibacterial activity of optimized hydrogel. Standard agar well diffusion method was used to determine the antibacterial activity of the optimized hydrogel. Nutrient agar was prepared, autoclaved and allowed to solidify at room temperature. The autoclaved agar plates were inoculated with bacterial cell suspensions. Wells (8 mm) were made in each agar plate using a sterile metallic borer. To each well, 80 μL of the sample was loaded in serial dilutions (2.5, 5, 10 and 20 $\mu\text{g}/\text{mL}$). Similarly, 80 μL of ciprofloxacin was added in serial dilutions as positive control. All the plates were incubated at 37 °C for 24 h and the results were expressed as a zone of inhibition in mm [39].

The minimum inhibitory concentration (MIC) of the prepared optimized hydrogel was determined by a serial twofold dilution of test samples. Different concentrations (2.5, 5, 10 and 20 $\mu\text{g}/\text{mL}$) of the hydrogel were prepared in autoclaved distilled water. 10 μL of the bacterial strain was inoculated to each tube containing different concentrations (1 mL) of the prepared hydrogel and incubated at 37 °C (250 rpm) for 24 h. The MIC was defined as the minimum concentration of the sample inhibiting the visible growth of the microorganism [40].

Table 2 Flory–Huggins network parameters of gelatin/CMC hydrogels

Sample code	* $V_{2,s}$	** χ	*** M_c	**** N
S1	0.102559	0.53705	553.2698	2.880767
S2	0.122849	0.54514	538.0713	2.814286
S3	0.145998	0.54801	327.149	1.638542
S4	0.134718	0.54999	299.0155	1.563035
S5	0.098798	0.53558	587.7291	3.062969
S6	0.083578	0.52973	770.9455	4.008429
S7	0.100421	0.53622	505.2325	2.63391
S8	0.125865	0.54636	411.7194	2.153978
S9	0.129459	0.55156	336.3217	1.754317

*Volume fraction of polymer in the swollen state ($V_{2,s}$), **Solvent interaction parameters (χ), ***Molecular weight among crosslinking junctions (M_c), ****The number of links between two crosslinks (N)

Antifungal assay

Four pathogenic fungi, *Mucor species* (FCBP 0300), *Aspergillus fumigatus* (ATCC 204,305), *Cryptococcus* (ATCC 90113) and *Candida Albicans* (ATCC 90028), were studied by the agar dilution method with some modification. The autoclaved *Potato Dextrose Agar* (PDA) media with optimized hydrogel at concentrations 2.5, 5, 10 and 20 $\mu\text{g/mL}$ were poured into the petri dishes (9 cm diameter). The fungi were inoculated after the PDA media solidified. A disc (1.4 cm) of mycelial material taken from the edge of 7-day-old fungal cultures was placed in the centre of each petri dish. The Petri dish with the inoculums was then incubated at 25 °C. The efficacy of optimized hydrogels was evaluated at the time intervals of 0, 2, 4, 8, 10, 12, 24, 48 and 72 h by measuring the diameter of fungal colonies. Fluconazole was used as control. We performed all tests in triplicate and expressed the values in millimetres [41].

Results and discussion

Structural parameters of hydrogel

The results of Table 2 demonstrate the values of various structural parameters of prepared hydrogels. It was observed that values of $V_{2,s}$ and χ increased with an increase in concentration of CMC and GA whereas reverse has been observed for gelatin. Values of M_c and N decreased with an increase in concentration of CMC and GA and increased by increasing amount of gelatin. Reason behind this was increase in crosslinking density with an increase in amount of CMC and GA leading to decrease in M_c and N . Increase in $V_{2,s}$ and χ with an increase in amount of CMC and GA and decrease in amount of gelatin indicates the increased swollen polymer [42].

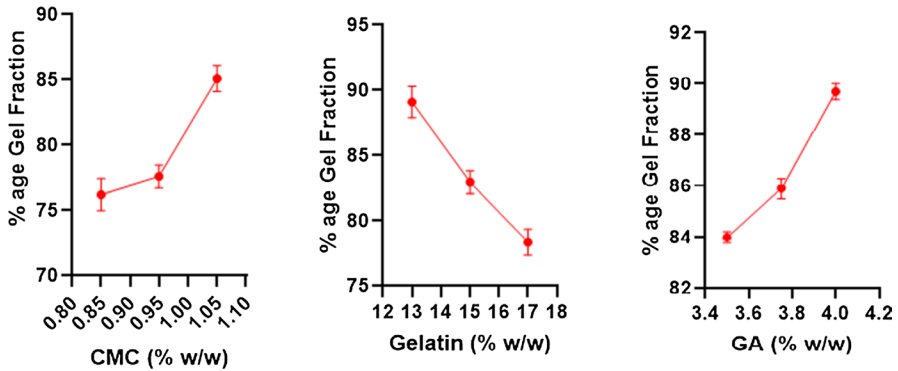


Fig. 2 Effects of CMC, gelatin and GA concentration on gel fraction of hydrogels

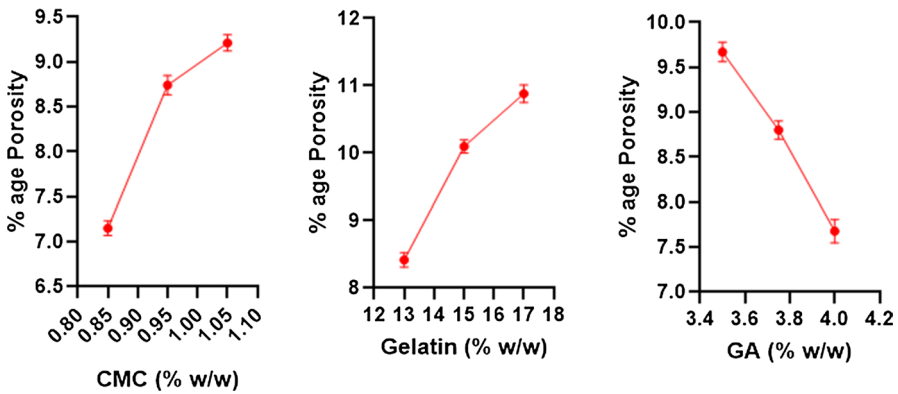


Fig. 3 Effect of CMC, gelatin and GA concentration on porosity of hydrogels

Sol–gel analysis

Sol–gel fraction of all samples was calculated to elaborate the effect of different concentrations of polymers and crosslinker on gel strength. It was observed that gel fraction increased with an increase in concentration of CMC and GA while decreases with increase in concentration of gelatin. The results of Fig. 2 show the effect of different concentrations of gelatin, CMC and GA on gel fraction, respectively. Gel fraction is directly related to crosslinking density; therefore, it can be concluded that increase in concentration of CMC and GA led to an increase in gel strength whereas increase in gelatin concentration may reduce the crosslinking reaction and consequently the gelation process is clearly reduced [43].

Porosity

Percentage porosity of all samples was calculated to elaborate the effect of different concentrations of gelatin, CMC and GA on porosity of hydrogels. The results of Fig. 3 show the effect of different concentrations of gelatin, CMC and GA on porosity of hydrogels, respectively [44]. It was noticed by increasing the concentration of gelatin and CMC, porosity of hydrogels increases, while with an increase in concentration of GA, porosity decreases. Porous structure might also be due to the presence of ionic and hydrophilic groups in developed polymeric network, i.e. CMC and gelatin. Therefore, incorporating the hydrophilic component in the hydrogel structure might have increased the system hydrophilicity and subsequently porosity of hydrogels. Increase in GA concentration increased the crosslinking density and physical entanglement between gelatin and CMC, which in turn caused decrease in porosity [45].

Fourier transform infrared spectroscopy (FTIR)

FTIR spectral data were used to confirm the crosslinking of gelatin and CMC chains by GA as shown in Fig. 4. In the case of gelatin, a characteristic band due to N–H stretching is observed at 3416 cm^{-1} . The N–H bending vibration is assigned to band observed at 1402 cm^{-1} . Aliphatic C–H stretching is observed at 2926 cm^{-1} , while aliphatic C–H bending vibrations are observed at 1450 and 1402 cm^{-1} . The band appearing at 1638 cm^{-1} indicates amide I band, while the band at 1327 cm^{-1} is assigned to the C–N bond stretching vibrations. Na CMC shows bands at 3400 and 3200 cm^{-1} due to O–H stretching vibration. The distant band at 2986 cm^{-1} shows aliphatic C–H stretching vibrations, but those appearing at 1519.91 and 1319.21 cm^{-1} are due to the asymmetric and symmetric stretching of the carboxylate group, respectively. Gelatin/CMC hydrogel shows the new bands at 1118 and 1060 cm^{-1} represent C–O–C stretching vibrations, which confirmed the crosslinking of polymers. Some of the characteristic bands of ciprofloxacin HCl appeared in the ciprofloxacin-loaded hydrogel (curve e), suggesting the successful loading of drug in hydrogel [46, 47].

Differential scanning calorimetry (DSC)

DSC thermograms of pure drug-unloaded and drug-loaded hydrogels are presented in Fig. 5. Thermogram of DSC clearly indicates melting peak of ciprofloxacin HCl at about $250\text{ }^{\circ}\text{C}$. Both drug-loaded and -unloaded hydrogels showed a melting peak at $40\text{ }^{\circ}\text{C}$ which is attributed to melting of gelatin (main component of hydrogel structure). The drug-loaded hydrogel showed an absence of drug melting peak which indicates molecular dispersion of drug in prepared hydrogels. The unloaded sample did not show any endothermic transitions due to rigid polymer network structure because of chain entanglement [48].

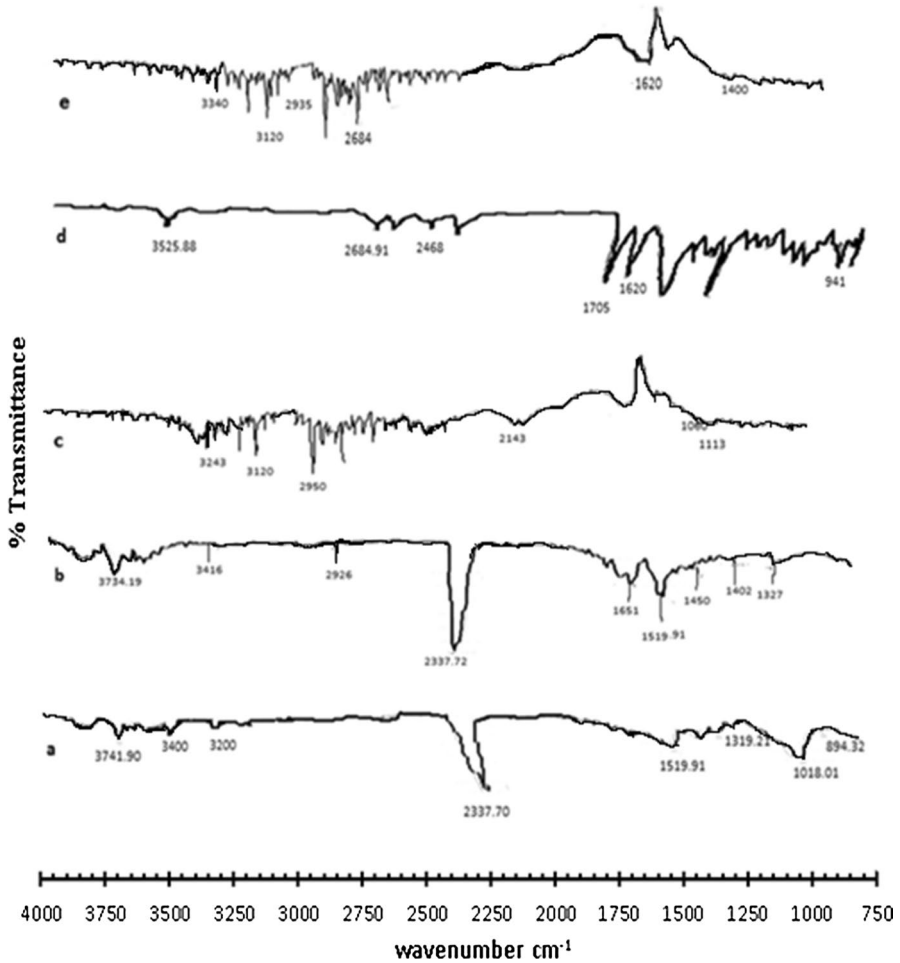


Fig. 4 FTIR spectra for CMC **a**, gelatin **b**, gelatin/CMC hydrogel **c**, ciprofloxacin HCl **d** and drug-loaded hydrogel **e**

X-ray diffraction (XRD)

XRD patterns of drug, gelatin/CMC hydrogel and drug-loaded gelatin/CMC hydrogel are presented in Fig. 6. The blunt and prominent peaks in the XRD diffractogram of drug represent its crystalline state. The diffractogram of unloaded gelatin/CMC hydrogel indicated peaks at 2.354, 2.035, 1.437, 1.355 and 1.224° (2 theta). The diffractogram of drug-loaded gelatin/CMC hydrogel indicated peaks at 2.355, 2.038, 1.438, 1.357 and 1.225° (2 theta). Peaks of unloaded and drug-loaded hydrogel are nearly same, which means that there is no apparent interaction reported between drug and hydrogel. Moreover, the crystallinity of

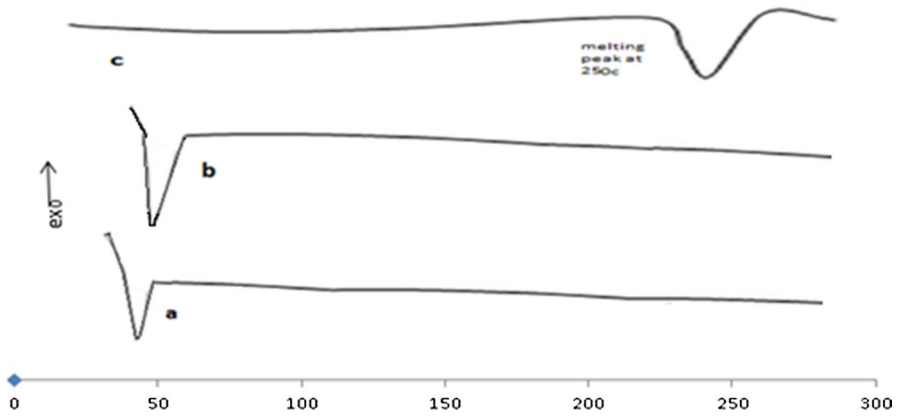


Fig. 5 DSC thermogram of gelatin/CMC hydrogel **a**, drug-loaded hydrogel **b** and ciprofloxacin HCl **c**

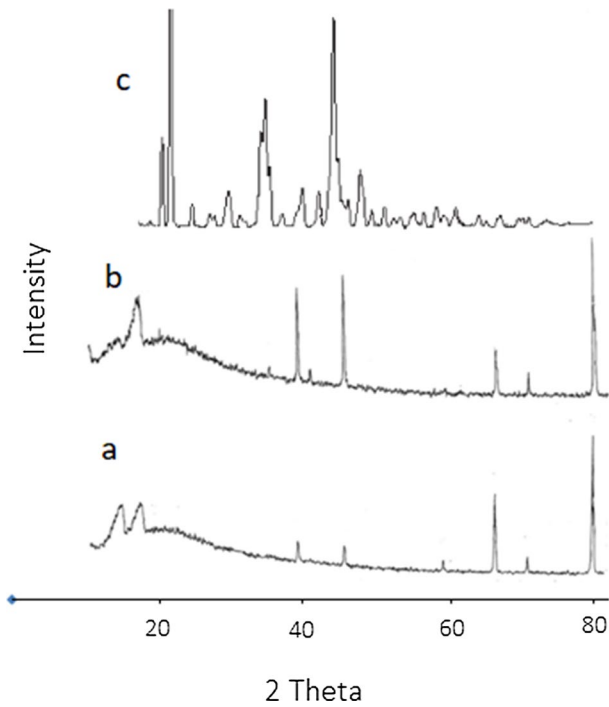


Fig. 6 XRD for gelatin/CMC hydrogel **a**, drug-loaded hydrogel **b**, ciprofloxacin HCl **c**

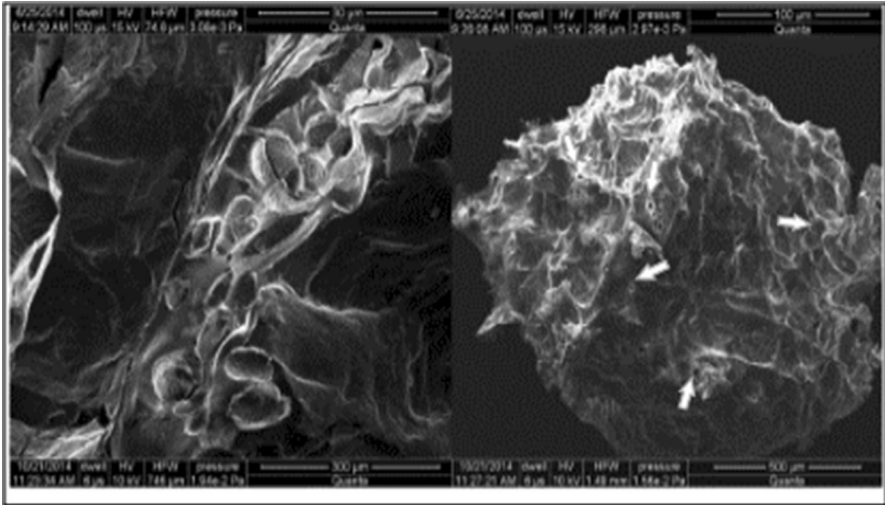


Fig. 7 SEM image of hydrogel

Table 3 Dynamic and equilibrium swelling ratios of hydrogels at pH 1.2, pH 5.5 and pH 7.4

S. no.	Dynamic swelling ratio			Equilibrium swelling ratio		
	pH 1.2	pH 5.5	pH 7.4	pH 1.2	pH 5.5	pH 7.4
S1	5	4.08	3.27	11.53	5.25	4.41
S2	4.48	3.73	3.35	11.37	4.87	4.5
S3	4.47	3.66	3.59	11.1	4.8	4.63
S4	4.67	3.66	3.39	9.65	4.89	4.49
S5	4.75	3.74	3.43	12.06	4.92	4.57
S6	5.27	4.38	3.54	14.7	6.00	4.60
S7	4.48	3.74	3.47	13.2	4.75	4.59
S8	4.01	3.26	3.12	11.6	4.48	4.12
S9	3.67	3.11	2.78	10.7	4.00	3.50

drug decreased following its loading which is an indication of successful encapsulation and dispersion at molecular level in hydrogel structure [49].

Scanning electron microscopy

Surface morphology of both drug-loaded and plain gelatin/CMC hydrogels is shown in Fig. 7. Hydrogels possessed a highly porous structure, responsible for swelling behaviour, drug loading and drug release through diffusion from these pores. Arrows in Fig. 7 indicates the presence of pores in developed hydrogel.

Swelling dynamics of gelatin/CMC hydrogels

Effect of pH and reactants concentration

The results of Table 3 show the dynamic and equilibrium swelling ratio of gelatin/CMC hydrogels. It is clear from the table that swelling ratio decreased by increasing the pH of medium, secondly, increasing the concentration of gelatin increased the swelling ratio at all pH values and thirdly, increasing the amount of CMC decreased the swelling ratio at lower pH (1.2 and 5.5), while at higher pH (7.4) increasing CMC content increased the swelling ratio. This may be due to following reasons; (i) At lower pH values, free NH_2 groups of gelatin are protonated resulting in electrostatic repulsion between NH_3^+ groups which in turn expansion of polymer network, on the other hand, free COOH groups with hydroxyl groups of CMC form lactone ring and cause contraction of polymer network [50]; (ii) At higher pH value carboxylic groups of CMC become ionized and electrostatic repulsion between carboxylate groups ($-\text{COO}^-$) causes expansion of polymer network [38]. The effect of gelatin on swelling ratio was more prominent than CMC due to a greater weight ratio of gelatin to CMC in hydrogels, therefore swelling ratio of hydrogel decreased with increase in pH value and maximum swelling was observed at pH 1.2.

Influence of CMC concentration on swelling of hydrogels

To elaborate the effect of concentration of CMC on swelling of hydrogel, three hydrogel samples (S_1 , S_2 and S_3) were prepared with varying concentration of CMC (0.85, 0.95 and 1.05 g) and keeping the concentration of gelatin and GA constant. At lower pH values (1.2 and 5.5) swelling ratio decreased with increasing concentration of CMC, while at pH 7.4 swelling ratio increased with increasing amount of CMC. Increase in swelling at higher pH due to electrostatic repulsion of carboxylate groups and increase in CMC concentration cause decrease in swelling at lower pH due to protonation of carboxylate groups. At acidic pH, CMC possess free carboxylic and hydroxyl groups, they form lactone ring and cause contraction of network. Strong hydrogen interactions also occur between free carboxylic groups of CMC and free hydroxyl groups of CMC and gelatin leading to crosslinking and contraction of network [51].

Influence of gelatin concentration on swelling of hydrogels

Figure 8 shows the impact of gelatin concentration on dynamic swelling behaviour of hydrogels. All samples (S_4 , S_5 and S_6) were prepared with varying concentration of gelatin (13, 15 and 17 g) and keeping the concentration of CMC and GA constant showed increase in swelling with increasing concentration of gelatin in solutions of pH values (1.2, 5.5 and 7.4). This can be related that at lower pH values free amino groups of gelatin are protonated and electrostatic repulsion occurs between them leading to relaxation of polymer network while at higher pH (7.4) ionization of carboxylic groups of gelatin causes expansion of network; therefore, at all pH

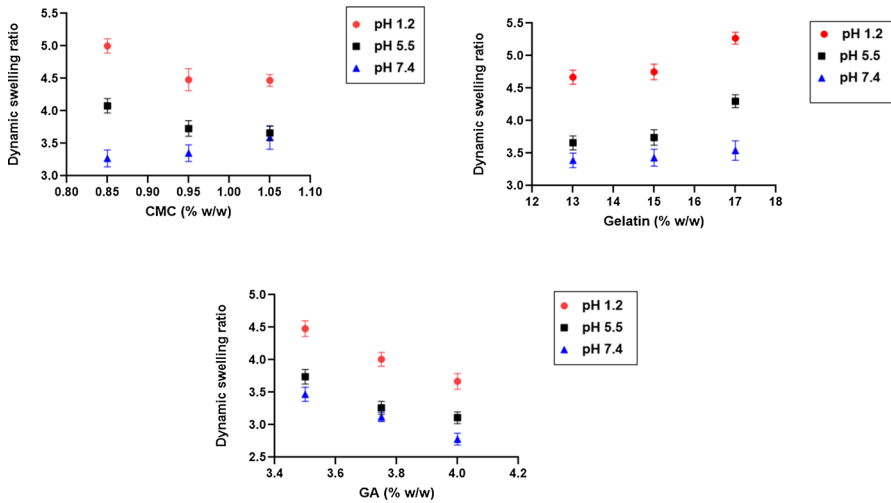


Fig. 8 Effect of different concentrations of reactants on dynamic swelling ratio of hydrogels at different pH values (1.2, 5.5 and 7.4)

values swelling ratio increased with increase in gelatin. Moreover, gelatin is more hygroscopic than CMC because of having higher number of polar groups [52]. This difference in water affinity caused the gelatin to be mainly responsible for swelling of hydrogel.

Impact of GA concentration on swelling of hydrogels

To investigate the effect of concentration of GA on swelling of hydrogels, three samples (S_7 , S_8 and S_9) were studied with different concentrations of GA (3.5, 3.75 and 4 g) keeping the concentration of both polymers constant. The results of Fig. 8 show the impact of concentration of GA on dynamic swelling ratio of gelatin/CMC hydrogel. These results indicate that swelling ratio decreased by increasing concentration of GA from 3.5 to 4% of polymers. This is due to increase in crosslinking density and decrease in mesh size. With increase in concentration of crosslinker, the force by which GA binds with gelatin and CMC also increases leading to increase in mechanical strength of hydrogel [53]. It results in more tight and hard structure of hydrogel which in turn decreases water uptake capacity of polymer network leading to decrease in swelling degree.

Drug entrapment efficiency (DEE) and drug release behaviour

%DEE and drug release behaviour of developed hydrogels at both pH 1.2, 5.5 and 7.4, respectively, are shown in Table 4. Drug loading efficiency (%DEE) has been found to be oscillating within 63–85%. Moreover, the data tabulated in Table 4 also indicate that the hydrogel formulation which have shown maximum swelling ratio

Table 4 Percentage release of ciprofloxacin HCl from gelatin/CMC hydrogels

Sample code	Drug entrapment efficiency (DEE)	(% Amount of ciprofloxacin HCl released)		
		pH 1.2	pH 5.5	pH 7.4
S1	69	61.56	50.19	41.87
S2	67	60.11	49.00	40.77
S3	63	58.04	45.90	39.32
S4	72	68.02	51.35	44.13
S5	80	73.94	55.64	42.66
S6	85	76.83	58.02	39.27
S7	76	69.28	56.81	45.87
S8	70	61.34	53.1	41.93
S9	66	56.02	49.38	36.71

exhibited the highest loading efficiency for drug and ultimately per cent release of drug. Moreover, it is clear from Fig. 9 that drug release decreased by increasing the pH of medium, similar to swelling dynamics. This trend is consistent with all hydrogels which is shown in Fig. 9 [54].

When hydrogel discs are immersed in water, water enters into polymer network by diffusion due to osmotic pressure gradient. This diffusion of water causes the discs to swell and release the loaded drug. Evaluation of method that best fits the release data was done by considering regression coefficient. The results of Table 5 show the values of regression coefficient (r) of samples. These samples also showed zero-order release because of greater value of r for zero-order release. Values of regression coefficient (r) for Higuchi model of samples with varying concentration of gelatin (S_4, S_5, S_6) and varying concentration of GA (S_7, K_8, K_9) revealed that drug

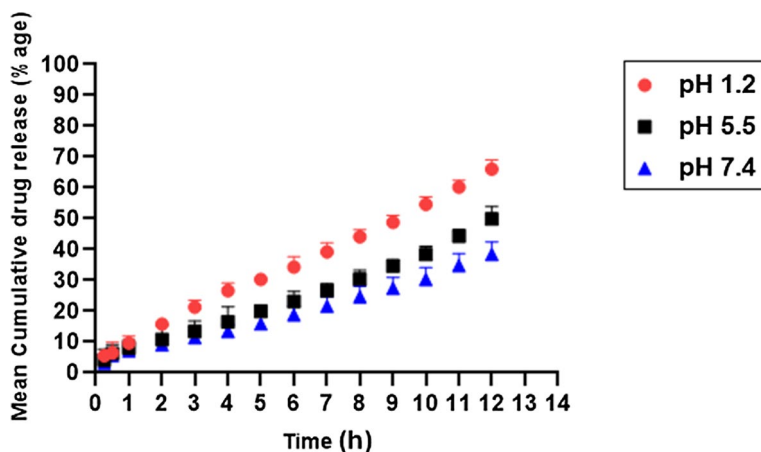
**Fig. 9** Mean cumulative drug release at pH 1.2, pH 5.5, pH 7.4

Table 5 Release kinetics of ciprofloxacin HCl from gelatin/CMC hydrogels

Sample code	pH	Zero-order kinetics		First-order kinetics		Higuchi Model	
		K_0 (h^{-1})	r	K_1 (h^{-1})	r	K_2 (h^{-1})	R
S1	1.2	3.644	0.998	0.037	0.959	0.156	0.963
	5.5	4.066	0.967	0.051	0.965	0.176	0.941
	7.4	3.443	0.999	0.037	0.980	0.130	0.925
S2	1.2	3.456	0.977	0.021	0.959	0.194	0.943
	5.5	2,879	0.988	0.061	0.985	0.148	0.921
	7.4	3.567	0.995	0.038	0.990	0.22	0.945
S3	1.2	4.211	0.999	0.043	0.989	0.194	0.955
	5.5	2.987	0.989	0.021	0.965	0.168	0.964
	7.4	3.678	0.996	0.065	0.964	0.123	0.954
S4	1.2	5.332	0.993	0.068	0.987	0.204	0.989
	5.5	3.924	0.990	0.046	0.989	0.153	0.986
	7.4	2.707	0.977	0.027	0.954	0.097	0.907
S5	1.2	5.768	0.998	0.058	0.974	0.186	0.975
	5.5	4.173	0.998	0.035	0.977	0.127	0.972
	7.4	3.150	0.997	0.027	0.987	0.103	0.980
S6	1.2	5.826	0.996	0.030	0.974	0.109	0.989
	5.5	4.359	0.995	0.037	0.963	0.119	0.965
	7.4	3.320	0.995	0.065	0.974	0.181	0.944
S7	1.2	5.355	0.996	0.044	0.974	0.153	0.964
	5.5	4.524	0.995	0.036	0.968	0.132	0.951
	7.4	3.577	0.997	0.029	0.981	0.109	0.956
S8	1.2	4.834	0.998	0.040	0.985	0.146	0.981
	5.5	4.310	0.997	0.033	0.982	0.125	0.967
	7.4	3.311	0.983	0.021	0.956	0.087	0.939
S9	1.2	4.644	0.998	0.067	0.989	0.194	0.963
	5.5	4.090	0.988	0.055	0.965	0.168	0.915
	7.4	3.132	0.995	0.038	0.990	0.130	0.945

release mechanism is diffusion controlled. Plot between fraction of drug release and square root of time was linear, which indicated diffusion-controlled release [55].

Values of release exponent (n) for Korsmeyer–Peppas model of all drug-loaded samples were between 0.5 and 1, which indicated non-Fickian diffusion. The results of Table 6 show the values of release exponent (n) of samples.

Biological activities

On the basis of maximum drug entrapment efficiency and in vitro cumulative drug release, one optimized hydrogel formulation, S6, was chosen for biological evaluation.

Table 6 Release mechanism of ciprofloxacin HCl from gelatin/CMC hydrogels

Sample code	pH	<i>r</i>	Release exponent (<i>n</i>)	Order of release
S1	1.2	0.955	0.766	Non-Fickian
	5.5	0.981	0.678	Non-Fickian
	7.4	0.976	0.787	Non-Fickian
S2	1.2	0.956	0.856	Non-Fickian
	5.5	0.934	0.821	Non-Fickian
	7.4	0.987	0.756	Non-Fickian
S3	1.2	0.967	0.761	Non-Fickian
	5.5	0.956	0.699	Non-Fickian
	7.4	0.901	0.865	Non-Fickian
S4	1.2	0.989	0.869	Non-Fickian
	5.5	0.982	0.781	Non-Fickian
	7.4	0.942	0.686	Non-Fickian
S5	1.2	0.981	0.841	Non-Fickian
	5.5	0.985	0.770	Non-Fickian
	7.4	0.989	0.718	Non-Fickian
S6	1.2	0.985	0.807	Non-Fickian
	5.5	0.901	0.638	Non-Fickian
	7.4	0.946	0.659	Non-Fickian
S7	1.2	0.990	0.818	Non-Fickian
	5.5	0.987	0.830	Non-Fickian
	7.4	0.981	0.779	Non-Fickian
S8	1.2	0.979	0.965	Non-Fickian
	5.5	0.989	0.997	Non-Fickian
	7.4	0.979	0.984	Non-Fickian
S9	1.2	0.984	0.907	Non-Fickian
	5.5	0.961	0.978	Non-Fickian
	7.4	0.976	0.998	Non-Fickian

Antioxidant assay

Antioxidant activity of optimized (S6) hydrogels was determined by DPPH scavenging assay by using ascorbic acid as standard. DPPH (1,1-diphenyl-2-picryl-hydrazil) was a stable free radical compound and have the ability to accept electrons. The results confirmed efficient free radical inhibition by optimized hydrogel (S6) in Fig. 10. Eleven different concentrations of S6 hydrogel were studied, and the outcome of antioxidant activity increased with increasing concentrations of hydrogels thus showing increased free radical scavenging effect in a dose-dependent manner. The IC₅₀ of S6 hydrogel was 211 µg/mL, while for ascorbic acid it was 434 µg/mL showing more potent antioxidant potentials even at lower concentrations [56].

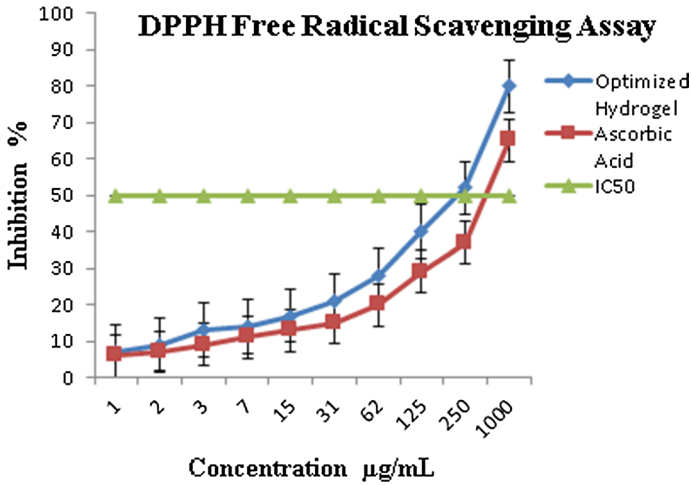


Fig. 10 Antioxidant potential of optimized hydrogel (S6)

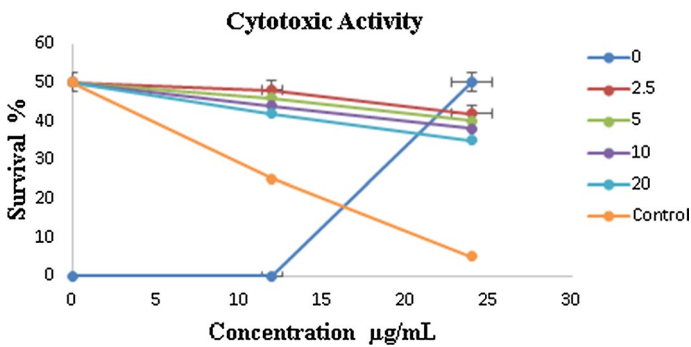


Fig. 11 Cytotoxic potential of optimized hydrogel (S6)

Cytotoxic assay

After 24 h exposure, the brine shrimp viability was evaluated. The S6 hydrogel was found to be biocompatible with the newly hatched larvae of *Artemia salina* up to concentration of 20 $\mu\text{g/mL}$. Maximum mortality was observed at highest concentration of 250 $\mu\text{g/mL}$. Moreover, the outcomes confirmed no dose-dependent reduction on viability up to 150 $\mu\text{g/mL}$ on exposure to S6 hydrogel when compared with the control. The absence of any significant toxicity of S6 hydrogel concludes that developed hydrogel is biocompatible below 150 $\mu\text{g/mL}$ [57] which is clearly indicated in Fig. 11.

Antibacterial assay

The antibacterial activity of the optimized hydrogel was tested against both gram-positive (*S. aureus*, *S. pneumoniae*) and gram-negative (*P. aeruginosa*, *Klebsiella*

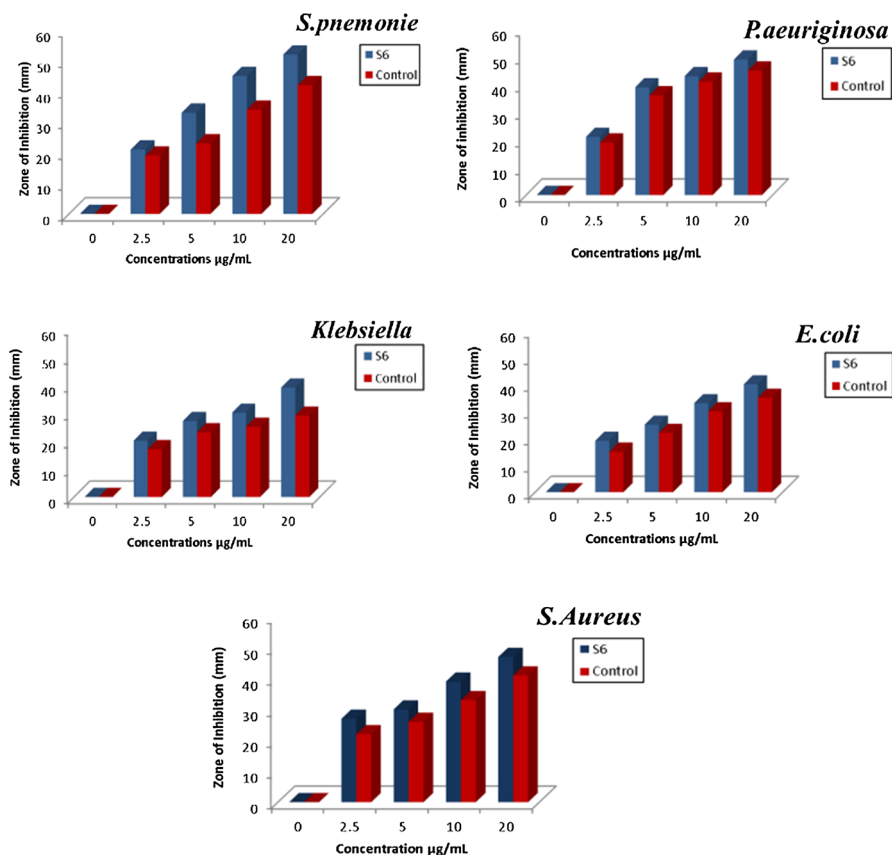


Fig. 12 Antibacterial activity of optimized hydrogel (S6) against different bacterial strains

Table 7 Antibacterial potential of optimized hydrogel (S6) against gram-positive and gram-negative bacterial strains

Bacteria	Control		Sample	
	Zone of inhibition (mm)	MIC (µg/mL)	Zone of inhibition (mm)	MIC (µg/mL)
<i>S. pneumoniae</i>	22 ± 1.2	3.125	26 ± 1.2	3.125
<i>S. aureus</i>	18 ± 1.1	3.125	22 ± 1.1	3.125
<i>P. aeruginosa</i>	17 ± 0.8	6.25	19 ± 0.8	6.25
<i>E. coli</i>	17 ± 0.8	6.25	18 ± 0.7	6.25
<i>Klebsiella</i>	19 ± 0.8	6.25	17 ± 0.5	6.25

and *E. coli*) bacterial strains. The results are expressed as a zone of inhibition Fig. 12. It was observed that S6 hydrogel exhibited significant activity against gram-positive strains with a zone of inhibition of 22 ± 1 mm, and 26 ± 1.2 for *S. aureus*

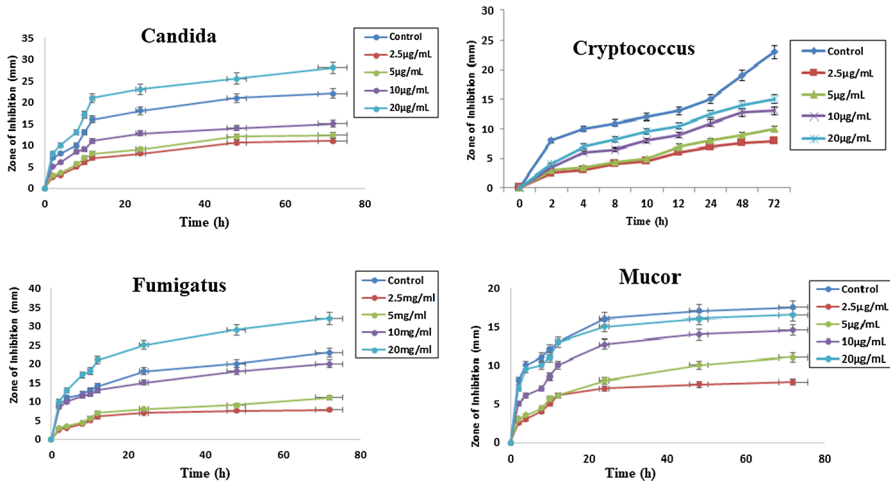


Fig. 13 Antifungal potentials of optimized hydrogel (S6) against different fungal stains

and *S. pneumoniae*, respectively (Table 7), even at lowest concentration of 2.5 µg/mL. However, the S6 hydrogel were relatively not as much active against the gram-negative strains just like aeruginosa, *E. coli* and *Klebsiella* with zones of inhibitions of 19 ± 0.8 , 18 ± 0.7 and 17 ± 0.5 mm, respectively, against the MIC concentration of 5 µg/mL but the results are still comparable to the parent drug which show no loss of activity even in the case when activity is not significantly improved. This could be explained by difference in polarity and charge of microorganisms outer membrane between gram-positive and gram-negative bacteria. The low activity of hydrogel against the gram-negative strains might be credited to the dissimilarity in the cell wall composition among the gram-positive and gram-negative bacteria. The cell wall of gram-negative strains is enclosed with an external lipid membrane (lipopolysaccharide) which is extra negatively charged than positive strains. The effectiveness of these hydrogel was further confirmed by determining the minimum inhibitory concentrations against the used bacterial strains. The hydrogels exhibited MIC value of 5 and 10 µg/ml against the gram-positive and gram-negative strains, respectively. Our findings point towards hydrogels being more efficient in arresting bacterial growth. This result indicates that hydrogels could be used successfully to treat the emerging microbial resistance [58].

Antifungal assay

Figure 13 shows the effect of optimized hydrogel (S6) on the growth of *Mucor*, *A. fumigatus*, *Cryptococcus* and *Candida* that were cultivated on PDA containing different concentrations of optimized hydrogel (2.5, 5, 10 and 20 µg/mL) and incubated at 25 °C. The obtained results showed that it inhibited fungal growth for all of the fungal strains, *Mucor*, *A. fumigatus*, *cryptococcus* and *Candida* at different concentrations and the inhibition was dependent on the species tested. The lowest growth inhibition was obtained against *cryptococcus* at the hydrogel concentration of 5 ug/mL, whereas

the highest growth inhibition was obtained against *A. fumigatus* and *Candida* at the hydrogel concentration of 5 $\mu\text{g/mL}$. Moreover, there is no significant increase in growth inhibition against *cryptococcus* on increasing the concentration of hydrogels from 5 to 10 and 20 $\mu\text{g/mL}$, respectively. For *candida*, optimized hydrogel (S6) exhibited antifungal activity pattern comparable to *A. fumigatus* at the hydrogel concentration of 2.5, 5, 10 and 20 $\mu\text{g/mL}$. For *fumigates* and *candida*, there is almost twofold increase in fungal growth inhibition as the concentration of hydrogels increased from 5 to 20 $\mu\text{g/mL}$. Moreover, no significant growth inhibition was observed from 48 to 72 h and this pattern was consistent in all strains. Antifungal activity of developed S6 formulation against *A. fumigatus* and *Candida* was significantly higher than control. In case of *Mucor*, the growth inhibition was obtained at the hydrogel concentration of 10 $\mu\text{g/mL}$. There is concentration dependent increase in growth inhibition on increasing the concentration of hydrogel from 5 to 10 and 20 $\mu\text{g/mL}$, respectively. However, the highest concentration of S6 hydrogel i.e. 20 $\mu\text{g/mL}$, was found to be less effective against *Mucor* when compared with control. Hence, it can be said that optimized hydrogel (S6) is more effective against *fumigatus* and *Candida* and relatively less effective against *Mucor* and *cryptococcus* as compared to control [59].

Conclusion

Gelatin/CMC hydrogels have been synthesized using GA as crosslinking agent. Prepared hydrogels showed excellent sensitivity to pH of medium. Both swelling and drug release decreased by increasing pH and highest swelling ratio and maximum drug release was observed at pH 1.2. The results of drug release study suggested that release of model drug ciprofloxacin HCl was dependent on composition of gelatin/CMC hydrogels as well as pH of release medium. The results of release kinetic models suggested that model drug follows the zero-order release pattern and drug release mechanism was non-Fickian diffusion. Biological activity of optimized hydrogel indicated excellent antioxidant, antibacterial and antifungal activity, whereas cytotoxic assay indicated that developed hydrogel is non-toxic in nature. It can be concluded that this hydrogel based on gelatin and CMC has potential to be used as pH-sensitive drug delivery vehicle.

Funding No funding was received.

Declarations

Conflict of Interest The author(s) declare(s) that there is no conflict of interest regarding the publication of this article.

References

1. Zellweger RM, Carrique-Mas J, Limmathurotsakul D, Day NP, Thwaites GE, Baker S (2017) Southeast Asia antimicrobial resistance network. A current perspective on antimicrobial resistance in Southeast Asia. *J Antimicrob Chemother* 72(11):2963–2972

2. Collignon PJ, McEwen SA (2019) One health—its importance in helping to better control antimicrobial resistance. *Tropical Med Infect Disease* 4(1):22
3. Van Boeckel TP, Pires J, Silvester R, Zhao C, Song J, Criscuolo NG, Gilbert M, Bonhoeffer S, Laxminarayan R (2019) Global trends in antimicrobial resistance in animals in low- and middle-income countries. *Science* 365(6459):eaaw1944. <https://doi.org/10.1126/science.aaw1944>
4. Iqbal H, Khan BA, Khan ZU, Razzaq A, Khan NU, Menaab B, Menaab F (2020) Fabrication, physical characterizations and in vitro antibacterial activity of cefadroxil-loaded chitosan/poly (vinyl alcohol) nanofibers against *Staphylococcus aureus* clinical isolates. *Int J Biol Macromol* 144:921–931
5. Sharpe LA, Daily AM, Horava SD, Peppas NA (2014) Therapeutic applications of hydrogels in oral drug delivery. *Expert Opin Drug Deliv* 11(6):901–915
6. Yang K, Han Q, Chen B, Zheng Y, Zhang K, Li Q, Wang J (2018) Antimicrobial hydrogels: promising materials for medical application. *Int J Nanomed* 13:2217
7. Lima 2019, Studies on gelatin-based hydrogels with co-immobilized finibax and heparin for regenerative medicine. Kyushu University
8. Xu W, Dong S, Han Y, Li S, Liu Y (2018) Hydrogels as antibacterial biomaterials. *Curr Pharm Des* 24(8):843–854
9. Yu Y, Xu S, Li S, Pan H (2021) Genipin-cross-linked hydrogels based on biomaterials for drug delivery: a review. *Biomater Sci* 9(5):1583–1597
10. Sung YK, Kim SW (2020) Recent advances in polymeric drug delivery systems. *Biomater Res* 24(1):1–2
11. Birajdar MS, Joo H, Koh WG, Park H (2021) Natural bio-based monomers for biomedical applications: a review. *Biomater Res* 25(1):1–4
12. Sun B, Li C, Mao Y, Qiao Z, Jia R, Huang T, Xu D, Yang W (2021) Distinctive characteristics of collagen and gelatin extracted from *Dosidicus gigas* skin. *Int J Food Sci Technol* 56(7):3443–3454
13. Salvatore L, Gallo N, Natali ML, Terzi A, Sannino A, Madaghiele M (2021) Mimicking the hierarchical organization of natural collagen: toward the development of ideal scaffolding material for tissue regeneration. *Front in Bioeng Biotechnol* 9:644–595
14. Mad-Ali S, Benjakul S, Prodpran T, Maqsood S (2017) Characteristics and gelling properties of gelatin from goat skin as affected by drying methods. *J Food Sci Technol* 54(6):1646–1654
15. Dash R, Foston M, Ragauskas AJ (2013) Improving the mechanical and thermal properties of gelatin hydrogels cross-linked by cellulose nanowhiskers. *Carbohydr Polym* 91(2):638–645
16. Bello AB, Kim D, Kim D, Park H, Lee SH (2020) Engineering and functionalization of gelatin biomaterials: from cell culture to medical applications. *Tissue Eng Part B Rev* 26(2):164–180
17. Candido TM. Segurança e eficácia antioxidante pré-clínica e clínica de etosomas contendo rutina de orientação de uso cosmético (Doctoral dissertation, Universidade de São Paulo).
18. Rodríguez-Rodríguez R, Espinosa-Andrews H, Velasquillo-Martínez C, García-Carvajal ZY (2020) Composite hydrogels based on gelatin, chitosan and polyvinyl alcohol to biomedical applications: a review. *Int J Polym Mater Polym Biomater* 69(1):1–20
19. Skopinska-Wisniewska J, Tuszynska M, Olewnik-Kruszkowska E (2021) Comparative study of gelatin hydrogels modified by various cross-linking agents. *Materials* 14(2):396
20. Sethi S, Kaith BS, Kumar V (2019) Fabrication and characterization of microwave assisted carboxymethyl cellulose-gelatin silver nanoparticles imbibed hydrogel: Its evaluation as dye degradation. *React Funct Polym* 142:134–146
21. Pourjavadi A, Barzegar S, Mahdavinia GR (2006) MBA-crosslinked Na-Alg/CMC as a smart full-polysaccharide superabsorbent hydrogels. *Carbohydr Polym* 66(3):386–395
22. Malik NS, Ahmad M, Minhas MU, Murtaza G, Khalid Q (2017) Polysaccharide hydrogels for controlled release of acyclovir: development, characterization and in vitro evaluation studies. *Polym Bull* 74(10):4311–4328
23. Malik NS, Ahmad M, Minhas MU, Tulain R, Barkat K, Khalid I, Khalid Q (2020) Chitosan/xanthan gum based hydrogels as potential carrier for an antiviral drug: fabrication, characterization, and safety evaluation. *Front Chem* 8:50
24. Ghorpade VS, Yadav AV, Dias RJ, Mali KK, Pargaonkar SS, Shinde PV, Dhane NS (2018) Citric acid crosslinked carboxymethylcellulose-poly (ethylene glycol) hydrogel films for delivery of poorly soluble drugs. *Int J Biol Macromol* 118:783–791
25. Kim DW, Shchipunov Y, Kim GH, Shin I, Ha CS (2020) Effect of graphene oxide content on the tensile properties and swelling ratio of chitosan/xanthan gum/graphene oxide hydrogel films. *Mol Cryst Liq Cryst* 706(1):72–78


26. Saeed Abdelmonem Elqiey A (2020) Evaluation of antibacterial activity of chitosan-coated anisotropic silver Nanoparticles on different bacterial strains.
27. Sahraro M, Barikani M, Daemi H (2018) Mechanical reinforcement of gellan gum polyelectrolyte hydrogels by cationic polyurethane soft nanoparticles. *Carbohydr Polym* 187:102–109
28. Tiwari R, Krishnamoorthi S, Kumar K (2019) Synthesis of cross-linker devoid novel hydrogels: swelling behaviour and controlled urea release studies. *J Environ Chem Eng* 7(4):103162
29. Kanmaz N, Saloglu D, Hizal J (2019) Humic acid embedded chitosan/poly (vinyl alcohol) pH-sensitive hydrogel: Synthesis, characterization, swelling kinetic and diffusion coefficient. *Chem Eng Commun* 206(9):1168–1180
30. Sami AJ, Khalid M, Jamil T, Aftab S, Mangat SA, Shakoori AR, Iqbal S (2018) Formulation of novel chitosan guar gum based hydrogels for sustained drug release of paracetamol. *Int J Biol Macromol* 108:324–332
31. Peppas NA (ed) (1986) *Hydrogels in medicine and pharmacy*. CRC Press, Boca Raton, FL
32. Kumari PK, Sharmila M, Rao YS (2020) Super porous hydrogels: a review. *J Pharm Res Int* 32:153–165
33. Akhlaq M, Idrees N, Nawaz A, Jalil A, Zafar N, Adeel M, Ullah I, Mukhtiar M, Afridi HH (2020) HPMC-co-acrylic acid dexibuprofen once-daily oral hydrogels. *J Macromolec Sci, Part A* 57(9):663–674
34. Kour P, Afzal S, Gani A, Zargar MI, Tak UN, Rashid S, Dar AA (2022) Effect of nanoemulsion-loaded hybrid biopolymeric hydrogel beads on the release kinetics, antioxidant potential and antibacterial activity of encapsulated curcumin. *Food Chem* 376:131925
35. Wang H, Gong X, Guo X, Liu C, Fan YY, Zhang J, Niu B, Li W (2019) Characterization, release, and antioxidant activity of curcumin-loaded sodium alginate/ZnO hydrogel beads. *Int J Biol Macromol* 121:1118–1125
36. Javanbakht S, Shaabani A (2019) Carboxymethyl cellulose-based oral delivery systems. *Int J Biol Macromol* 133:21–29
37. Tong T, Deng S, Zhang X, Fang L, Liang J, Xiao S (2022) Inhibitory effect and mechanism of gelatin stabilized ferrous sulfide nanoparticles on porcine reproductive and respiratory syndrome virus. *J Nanobiotechnology* 20(1):1–3
38. Goudoulas TB, Vanderhaeghen S, Germann N (2022) Micro-dispersed essential oils loaded gelatin hydrogels with antibacterial activity. *LWT* 154:112797
39. Rahman M, Hasan M, Nitai AS, Nam S, Karmakar AK, Ahsan M, Shiddiky MJ, Ahmed MB (2021) Recent developments of carboxymethyl cellulose. *Polymers* 13(8):1345
40. Lordello VB, Meneguini AB, de Annunzio SR, Taranto MP, Chorilli M, Fontana CR, Cavallini DC (2021) Orodispersible film loaded with enterococcus faecium CRL183 presents anti-candida albicans biofilm activity in vitro. *Pharmaceutics* 13(7):998
41. Babaladimath G, Badalamoole V (2019) Silver nanoparticles embedded pectin-based hydrogel: a novel adsorbent material for separation of cationic dyes. *Polym Bull* 76(8):4215–4236
42. Nia SB, Pooresmaeil M, Namazi H (2020) Carboxymethylcellulose/layered double hydroxides bionanocomposite hydrogel: a controlled amoxicillin nanocarrier for colonic bacterial infections treatment. *Int J Biol Macromol* 155:1401–1409
43. Qi X, Yuan Y, Zhang J, Bulte JW, Dong W (2018) Oral administration of salectan-based hydrogels for controlled insulin delivery. *J Agric Food Chem* 66(40):10479–10489
44. Shariatnia Z (2018) Carboxymethyl chitosan: properties and biomedical applications. *Int J Biol Macromol* 120:1406–1419
45. Khan S, Anwar N (2021) Gelatin/carboxymethyl cellulose based stimuli-responsive hydrogels for controlled delivery of 5-fluorouracil, development, in vitro characterization, in vivo safety and bio-availability evaluation. *Carbohydr Polym* 257:117617
46. Esteghlal S, Niakousari M, Hosseini SM (2018) Physical and mechanical properties of gelatin-CMC composite films under the influence of electrostatic interactions. *Int J Biol Macromol* 114:1–9
47. Ghorpade VS, Dias RJ, Mali KK, Mulla SI (2019) Citric acid crosslinked carboxymethylcellulose-polyvinyl alcohol hydrogel films for extended release of water soluble basic drugs. *J Drug Deliv Sci Technol* 52:421–430
48. Zia MA, Sohail M, Minhas MU, Sarfraz RM, Khan S, de Matas M, Hussain Z, Abbasi M, Shah SA, Kousar M, Ahmad N (2020) HEMA based pH-sensitive semi IPN microgels for oral delivery; a rationale approach for ketoprofen. *Drug Dev Ind Pharm* 46(2):272–282
49. Malik NS, Ahmad M, Minhas MU (2017) Cross-linked β -cyclodextrin and carboxymethyl cellulose hydrogels for controlled drug delivery of acyclovir. *PLoS ONE* 12(2):e0172727

50. Ubaid M, Murtaza G (2018) Fabrication and characterization of genipin cross-linked chitosan/gelatin hydrogel for pH-sensitive, oral delivery of metformin with an application of response surface methodology. *Int J Biol Macromol* 114:1174–1185
51. Rakhshaei R, Namazi H, Hamishehkar H, Rahimi M (2020) Graphene quantum dot cross-linked carboxymethyl cellulose nanocomposite hydrogel for pH-sensitive oral anticancer drug delivery with potential bioimaging properties. *Int J Biol Macromol* 150:1121–1129
52. Sarrigiannidis SO, Rey JM, Dobre O, González-García C, Dalby MJ, Salmeron-Sanchez M (2021) A tough act to follow: collagen hydrogel modifications to improve mechanical and growth factor loading capabilities. *Materials Today Bio* 10:100098
53. Daud H, Ghani A, Iqbal DN, Ahmad N, Nazir S, Muhammad MJ, Hussain EA, Nazir A, Iqbal M (2021) Preparation and characterization of guar gum based biopolymeric hydrogels for controlled release of antihypertensive drug. *Arab J Chem* 14(5):103111
54. Manan FA, Yusof NA, Abdullah J, Mohammad F, Nurdin A, Yazan LS, Khiste SK, Al-Lohedan HA (2021) Drug release profiles of mitomycin c encapsulated quantum dots–chitosan nanocarrier system for the possible treatment of non-muscle invasive bladder cancer. *Pharmaceutics* 13(9):1379
55. Rai M, Ingle AP, Pandit R, Paralikar P, Anasane N, Santos CA (2020) Curcumin and curcumin-loaded nanoparticles: antipathogenic and antiparasitic activities. *Expert Rev Anti Infect Ther* 18(4):367–379
56. Eshkol-Yogev I, Kaufman A, Haddad M, Zilberman M (2022) Cell viability of novel composite hydrogels loaded with hydroxyapatite for oral and maxillofacial bone regeneration. *Odontology* 110(2):296–304
57. Ture H (2019) Characterization of hydroxyapatite-containing alginate–gelatin composite films as a potential wound dressing. *Int J Biol Macromol* 123:878–888
58. Marchesan S, Qu Y, Waddington LJ, Easton CD, Glattauer V, Lithgow TJ, McLean KM, Forsythe JS, Hartley PG (2013) Self-assembly of ciprofloxacin and a tripeptide into an antimicrobial nanostructured hydrogel. *Biomaterials* 34(14):3678–87
59. Sharma P, Chaudhary M, Khanna G, Rishi P, Kaur IP (2021) Envisaging antifungal potential of histatin 5: a physiological salivary peptide. *J Fungi* 7(12):1070

Publisher's Note Springer Nature remains neutral with regard to jurisdictional claims in published maps and institutional affiliations.

Springer Nature or its licensor (e.g. a society or other partner) holds exclusive rights to this article under a publishing agreement with the author(s) or other rightsholder(s); author self-archiving of the accepted manuscript version of this article is solely governed by the terms of such publishing agreement and applicable law.

Authors and Affiliations

Fariha Sahar¹ · Amina Riaz³ · Nadia Shamshad Malik²  · Nitasha Gohar² · Ayesha Rasheed³ · Ume Ruqia Tulain⁴ · Alia Erum⁴ · Kashif Barkat⁵ · Syed Faisal Badshah⁵ · Sayyed Ibrahim Shah⁶

¹ Faculty of Pharmacy, Bahauddin Zakariya University, Multan, Pakistan

² Faculty of Pharmacy, Capital University of Science and Technology, Islamabad, Pakistan

³ Department of Pharmacy, The Women University Multan, Multan, Pakistan

⁴ Faculty of Pharmacy, University of Sargodha, Sargodha, Pakistan

⁵ Faculty of Pharmacy, University of Lahore, Lahore, Pakistan

⁶ Department of Pharmacy, Abdul Wali Khan University, Mardan, Pakistan